Received: 5 September 2019 | Revised: 8 October 2019 | Accepted: 12 October 2019

DOI: 10.1002/aoc.5329

Applied Organometallic Chemistry WILEY

FULL PAPER

Synthesis, characterization and biological evaluation of *N*-substituted triazinane-2-thiones and theoretical–experimental mechanism of condensation reaction

Afsun Sujayev[1] | **Parham Taslimi**[2] | **Ruya Kaya**[3,4] | **Bahruz Safarov**[1] | **Lala Aliyeva**[1] | **Vagif Farzaliyev**[1] | **İlhami Gulçin**[3]

[1]Laboratory of Theoretical Bases of Synthesis and Action Mechanism of Additives, Institute of Chemistry of Additives, Azerbaijan National Academy of Sciences, 1029, Baku, Azerbaijan

[2]Department of Biotechnology, Faculty of Science, Bartin University, 74100, Bartin, Turkey

[3]Department of Chemistry, Faculty of Sciences, Ataturk University, 25240, Erzurum, Turkey

[4]Central Research and Application Laboratory, Agri Ibrahim Cecen University, 04100, Agri, Turkey

Correspondence
Parham Taslimi, Faculty of Science, Department of Biotechnology, Bartin University, 74100-.Bartin, Turkey.
Email: parham_taslimi_un@yahoo.com; ptaslimi@bartin.edu.tr

The synthesis of triazinthions and their reactions with some nucleophilic reagents have been investigated during this scientific study. Thus, thiourea with a single component has been synthesized as a result of concomitant reactions of aldehyde and amines trials. The structure of the synthesized compounds was confirmed by ^{1}H, ^{13}C NMR spectroscopy methods. The inhibitory effects of novel *N*-substituted triazinane-2-thione derivatives on acetylcholinesterase (AChE) activity were performed according to the spectrophotometric method of Ellman et al. These novel *N*-substituted triazinane-2-thiones derivatives were effective inhibitors of the α-glycosidase, cytosolic carbonic anhydrase I and II isoforms (hCA I and II), and Acetylcholinesterase (AChE) enzymes with K_i values in the range of 1.01 ± 0.28 to 2.12 ± 0.37 nM for α-glycosidase, 13.44 ± 4.39 to 74.98 ± 6.25 nM for hCA I, 10.41 ± 4.8 to 72.6 ± 17.66 nM for hCA II, 36.82 ± 9.95 to 108.48 ± 1.17 nM for AChE, and 624.62 ± 100.34 to 1124.16 ± 205.14 nM for α-glycosidase, respectively.

KEYWORDS

activation energy, enzyme inhibition, metabolic enzymes, *N*-substituted triazines

1 | INTRODUCTION

Among the heterocyclic compounds, triazine derivatives are attracting interest in medicinal and industrial chemistry and they are also being developed as a precursor for the synthesis of nitrogen-containing organic compounds. The triazine and hexahydrotriazine (triazinane) nuclei constitute well-known compounds that have been used as an anticonvulsant, anticoccidial, antiplasmodial, antimalarial and herbicidal agents. In addition, some of these compounds can serve as hydrogen sulfide scavengers, chiral discriminators and low-toxicity drug deliverers. Furthermore, heterocyclic compounds containing a thiourea or urea structural unit have a special place among pharmaceutically important natural and synthetic materials, showing powerful ectoparasiticidal action, potent antidiabetic properties and anti-HIV activity. A method of synthesis for 4,6-diphenyl-1,3,5-triazinane-2-thione was developed by three-component condensation of thiourea, benzaldehyde and ammonia.[1] Taking into consideration the above, we have continued to investigate the synthesis of new triazithione derivatives and their biological activity through triple-component condensation.

Carbonic anhydrase (CA, E.C.4.2.1.1) enzymes are very efficient enzymes, which catalyze the hydration of carbon dioxide to produce a proton and bicarbonate.[2–4] This mechanism is common for most organisms, and as an outcome of the evolution of

seven genetically varying families, this enzyme has also evolved to[5,6] α-CA enzymes. Sixteen different α-CA isozymes have been characterized and isolated in vertebrate and mammal cells so far, varying in cellular localization (mitochondria, cytosol, membrane) and tissue distribution.[7,8] Some isozymes have also been studied in detail by means of X-ray crystallography, recording images of the enzyme active site, where a zinc ion plays an axial role in the catalytic activity.[9] Indeed, other structural specifications of the enzyme active site have been highlighted, such as the presence of two diverse areas, one with hydrophilic amino acids and the other one lined with hydrophobic residues, offering the chance to modulate ligand design in disparate ways.[10,11] CA inhibitor compounds have been clinically used for almost 60 years as antiglaucoma and diuretics drugs.[12]

Acetylcholinesterase (AChE) is a significant enzyme that catalyzes the breakdown of acetylcholine (ACh) and some other choline ester molecules that function as neurotransmitter molecules, which are recorded as a drugs for Alzheimer's disease (AD).[13–16] The cholinergic hypothesis process was first proposed to describe AD and was based on the finding that the synaptic depression is hindered owing to the prevention of the ACh compound hydrolysis in the cholinergic neuron cells.[17,18] The inhibition action of AChE enzyme results in the blockage of ACh hydrolysis. Indeed, the design of inhibitor compounds or/and modulators for the AChE enzyme has been of major interest since it is customarily one of the best ways to prevent AD, resulting in three commercial drug compounds being approved by the US Food and Drug Administration, comprising rivastigmine, galantamine and donepezil.[19,20] Many potential inhibitors of AChE enzyme are under investigation, such as tacrine derivatives and Zijuan tea. Some of these derivatives are under clinical evaluation such as tacrine, huperzine A and ganstigmine.[21–24]

Recently, diverse hypoglycemic drug compounds have been utilized to lower the level of blood glucose in diabetic patients (like biguanides and sulfonylurea as well as other novel classes).[25,26] Between these classes are the inhibitor compounds of α-glycosidase – an enzyme which is accountable for the hydrolysis of carbohydrate molecules to facilitate the transmission of glucose molecules towards the blood compartment.[27] Presently, two kinds of drug compounds are utilized to inhibit the enzymatic activities of this enzyme in the intestine: the miglitol and the acarbose, which decrease postprandial hyperglycemia.[28] The inhibitor compounds of this enzyme not only have a beneficial effect on the postprandial glycaemia but also have a beneficial action against viral agents and arterial hypertension. Recent scientific research shows that various substances isolated from plant tissues have a very important hypoglycemic efficacy.[29]

In this study, we have performed a facile synthesis of the well-defined theoretical–experimental mechanism of the condensation reaction of novel *N*-substituted triazinane-2-thiones derivatives and also investigated their inhibition potential of cytosolic carbonic anhydrase I and II isoforms (hCA I and II), to discover the most favorable and potent AChE and α-glycosidase inhibition properties of these compounds.

2 | MATERIALS AND METHODS

2.1 | General chemistry

Solvents were distilled under anhydrous conditions. All reagents were purchased and used without further purification. Glassware was dried prior to use. Compounds were purified by dry flash chromatography using silica 60 < 0063 mm and water pump vacuum or by flash-chromatography using silica 60 Å 230–400 mesh as stationary phases. Thin-layer chromatography (TLC) plates (silica gel 60 F_{254}) were visualized either at a UV lamp or in iodine. Melting points are uncorrected. Elemental analysis was performed on the Carlo Erba 1108 analyzer.

2.2 | NMR experiments

NMR experiments were performed on a Bruker FT NMR spectrometer Avance 300 (300 MHz for ^{1}H and 75 MHz for ^{13}C) with BVT 3200 variable-temperature unit in 5 mm sample tubes using Bruker Standard software. The ^{1}H and ^{13}C chemical shifts were referenced to internal tetramethylsilane. NMR-grade DMSO-d_6 (99.7%, containing 0.3% H_2O) was used for the synthesized compounds.

2.3 | Kinetic approach

To illustrate the efficient catalytic route, the energetic span model (δG, here in terms of the Gibbs energy) was applied to demonstrate feasibility of the blue, orange and grey routes (see Figure 1). According to the energetic span model, the lowest energetic intermediate and the highest energetic transition state are determined for each route. The δG value was found to be the similar for blue (trifluoroacetic acid, TFA) and grey (acetic acid, AA) routes: 0.1 kcal/mol difference was observed. The δG value of the orange route (trichloroacetic acid, TCA) was

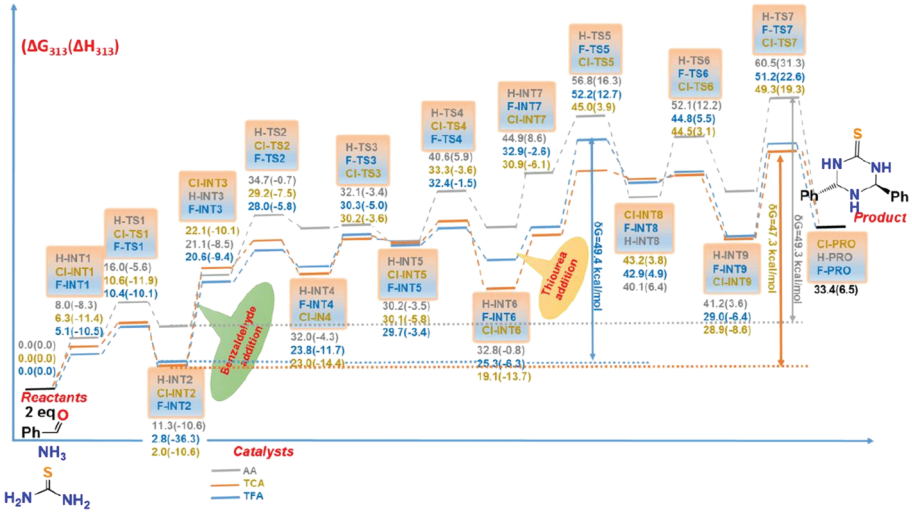

FIGURE 1 Reaction profile (kcal/mol) for the OTC triazinane-2-thione formation according to density functional theory (DFT) calculations. Blue, orange and grey colors correspond to the trifluoroacetic acid (TFA), trichloroacetic acid (TCA) and acetic acid (AA) catalyzed routes

2 kcal/mol less than the grey route. The TOF (turnover frequency) values were calculated for each route via using the Eyring equation (Equation (1)):

$$\mathrm{TOF} = \frac{k_B T}{h} e^{\frac{-\delta G}{RT}} \quad (1)$$

where k_B stands for Boltzmann's constant, h is Plank's constant, R is the universal gas constant and T is temperature in Kelvin. The following calculations [equations (2) and (3)] show us that there is no a dramatic difference in the catalytic efficiencies of TFA, TCA, and AA on the cyclocondenstation reaction:

$$\frac{\mathrm{TOF}_{\text{acetic acid}}}{\mathrm{TOF}_{\text{trifluoroacetic acid}}} = 1.17 \quad (2)$$

$$\frac{\mathrm{TOF}_{\text{trichloroacetic acid}}}{\mathrm{TOF}_{\text{acetic acid}}} = 24.91 \quad (3)$$

2.4 | Synthesis of new 4,6-disubstituted 1,3,5-Triazinane-2-thiones (1a–g)

2.4.1 | General procedure

The aldehydes (salicylic aldehyde, 4-methylbenzaldehyde, anisylaldehyde and benzaldehyde, 0.02–0.2 mol) were added to NH_4OH (33,5%, 15 ml) or amines (diethylenetryamine, methylamine and ethylamine, 0.01–0.05 mol) and the solution was stirred for 2–3 h at reflux. During this time, a white precipitate formed. The precipitate was removed by filtration and dried. The solid was dissolved in isopropyl alcohol (20 ml), thiourea (0.05–0.15 mol) was added to the mixture. Upon being dissolved in the stirring rod within 30 min the TFA catalyst was inserted. The resulting solution was stirred for 12–24 h at reflux. When the reaction mixture was cooled to room temperature, a white solid precipitated. The precipitates were filtered and recrystallized from Ethyl acetate (EtOAc) after dichloromethane washing and gave the product (4,6-disubstituted 1,3,5-triazinane-2-thiones, **1a**–**g**) in 65–85% yield.

2.4.2 | 5-(1,5-Diaminopentan-3-yl)-4,6-*bis*(2-hydroxyphenyl)-1,3,5-triazinane-2-thione (1a)

^{1}H NMR (300 MHz, DMSO-d_6, δ): d (mixture of two diastereoisomers) = 1.92 (t, J = 12.0 Hz, 1 H, NH), 2.0 m (2H, NH_2), 2.48, 2.65, 2.77, 2.81 (d, J = 7.75 Hz, 2H, CH_2), 3.03 (1H, NH), 5.04 (d, J = 12 Hz, 2H, 2CH–triazin), 6.61–7.04 (m, 20 H, CH–Ar), 7.31 (s, 1H, NH), 9.83 m (1H, PhOH).

^{13}C NMR (75 MHz, DMSO-d_6): d (single diastereoisomer, *trans*) = 36.5 (-CH_2), 57.7 (-CH_2), 70.3 (-CH–triazinane), 115.7, 119.9, 121.2, 128.5, 129.3 (-CH–Ar), 155 (-Ph–OH), 177.7 (-C=S).

2.4.3 | 5-Methyl-4,6-*bis*(*p*-tolyl)-1,3,5-triazinane-2-thione (1b)

^{1}H NMR (300 MHz, DMSO-d_6, δ): d (mixture of two diastereoisomers) = 2.0 (t, J = 11.5 Hz, 1H, NH), 2.19 (s, 6H, 2CH_3–Ar), 2.27 (s, 3H, CH_3–N), 5.04 (d, J = 12 Hz, 2H, 2CH–triazin), 6.94 (m, 8H, CH–Ar), 7.31 (br, 1H, NH).

^{13}C NMR (75 MHz, DMSO-d_6): d (single diastereoisomer, *trans*) = 24.3 (CH_3–Ar-), 32.7 (-N–CH_3), 79 (-CH–triazinane), 128.7, 135.3, 136.9 (-CH–Ar), 177.4 (C=S).

2.4.4 | 5-Ethyl-4,6-*bis*(2-hydroxyphenyl)-1,3,5-triazinane-2-thione (1c)

^{1}H NMR (300 MHz, DMSO-d$_6$, δ): d (single diastereoisomer, *trans*) = 1.00 (s, 3H, CH_3), 2.02 (t, J = 8.5 Hz, 1H, NH), 2.40 (d, J = 8.5 Hz, 2H, CH_2–N), 5.04 (d, J = 8.5 Hz, 2H, 2CH), 6.61, 6.70, 6.89, 7.04 (m, 1H, CH–Ar), 9.83 m (1H, OH).

^{13}C NMR (75 MHz, DMSO-d$_6$): d (single diastereoisomer, *trans*) = 13.3 (-CH_3), 38.8 (-CH_2–N-), 70.3 (-CH–triazinane), 115.6, 119, 121.1, 128.7, 130.2 (-CH–Ar), 155.9 (-Ph–OH), 177.6 (C=S).

2.4.5 | 4,6-Diphenyl-1,3,5-triazinane-2-thione (1d)

^{1}H NMR (DMSO-d$_6$, 300 MHz): d (mixture of two diastereoisomers) = 2.01 (t, J = 11.75 Hz, 1 H, NH), 2.55 (t, J = 8.75 Hz, 1 H, NH), 5.21 (d, J = 8.75 Hz, 2 H), 5.54 (d, J = 12 Hz, 2 H), 6.91 (s, 2 H, NH), 7.21 (s, 2 H, NH), 7.30–7.50 (m, 20 H).

^{13}C NMR (DMSO-d$_6$, 75 MHz): d (mixture of two diastereoisomers) = 65.7 (-CH–triazinane), 69.6 (-CH–triazinane), 126.4, 126.6, 128.9, 129.0, 129.2, 129.7, 137.1, 138.3 (-CH–Ar), 178.4 (C=S).

The compound (**1d**) was also synthesized according to above procedure and their ^{1}H- and ^{13}C-NMR data are in agreement with data given in the literature.[1]

2.4.6 | 5-Ethyl-4,6-*bis*(*p*-tolyl)-1,3,5-triazinane-2-thione (1e)

^{1}H NMR (300 MHz, DMSO-d$_6$, δ): d (mixture of two diastereoisomers) = 1.10 (t, 3H, CH_3), 1.94 (t, J = 12.0 Hz, 1H, NH), 2.19 (s 6H, 2CH_3–Ar), 2.40 (d, J = 6.0 Hz, 2H, CH_2–N-), 5.04 m (d, J = 12 Hz, 2H, 2CH), 6.9 (m 8H, CH–Ar).

^{13}C NMR (75 MHz, DMSO-d$_6$): d (single diastereoisomer, *trans*) = 15.5 (-CH_3), 22.4 (CH_3–Ar-), 24.3 (CH_3–Ar-), 39.5 (-CH_2–N-), 49 (-CH–triazinane), 74.8 (-CH–triazinane), 116.1, 127.8, 128.8, 129.3, 130.4, 136.2, 136.6, 138.3 (-CH–Ar), 182 (C=S).

2.4.7 | 5-Methyl-4,6-*bis*(4-methoxyphenyl)-1,3,5-triazinane-2-thione (1f)

^{1}H NMR (300 MHz, DMSO-d$_6$, δ): d (mixture of two diastereoisomers) = 2.27 (s, 3H, CH_3–N-), 2.30 (t, J = 12 Hz, 1 H, NH), 2.72 (t, J = 8.25 Hz, 1 H, NH), 3.72 (s, 6H, 2OCH_3), 5.02 (d, J = 8.25 Hz, 2H, 2CH), 6.65 (m, 4H, 2CH–Ar), 7.39 (m, 4H, 2CH–Ar).

^{13}C NMR (75 MHz, DMSO-d$_6$): d (single diastereoisomer, *trans*) = 32.7 (CH_3–N-), 55.7 (CH_3O-), 79 (-CH–triazinane), 114, 129.8, 130.6, 159.1 (-CH–Ar), 177.2 (C=S).

2.4.8 | 5-Ethyl-4,6-*bis*(4-methoxyphenyl)-1,3,5-triazinane-2-thione (1g)

^{1}H NMR (300 MHz, DMSO-d$_6$, δ): d (mixture of two diastereoisomers) = 1.01 (t, 3H, CH_3), 2.02 (t, J = 11.5 Hz, 1H, NH), 2.40 (s, 2H, CH_2–N-), 3.72 (s, 6H, 2OCH_3), 5.02 (d, 2H, 2CH), 6.65 (d, J = 11.5 Hz, 4H, 2CH), 7.39 (m, 4H, 2CH–Ar).

^{13}C NMR (75 MHz, DMSO-d$_6$): d (single diastereoisomer, *trans*) = 13.3 (-CH_3), 38.8 (-CH_2–N-), 55.8 (CH_3O-), 76.5 (-CH–triazinane), 114, 129.8, 130.6, 159.1 (-CH–Ar), 178 (C=S).

2.4.9 | 1,3-*bis*(2-Hydroxybutyl)-5-methyl-4,6-*bis*(*p*-tolyl)-1,3,5-triazinane-2-thione (2a)

5-Methyl-4,6-*bis*(*p*-tolyl)-1,3,5-triazinane-2-thion (**1b**) (3.11 g, 0.01 mol) was dissolved in a 2:1 ratio of acetylacetone and ethyl alcohol (12:5 ml) and 1,2-epoxobutane (2.03 ml, 0.02 mol) was added drop by drop. After being dissolved in the stirrer for 30 min, 0.02 g $AlCl_3$ catalyst was added and mixed by heating at 60–65°C. After determining the full completion of reaction, the solution was evaporated and cleaned in ethyl alcohol solution.

Analogously, 1,3-*bis*(2-hydroxypropyl)-5-methyl-4,6-*bis*(*p*-tolyl)-1,3,5-triazinane-2-thione (**2b**) was synthesized by the reaction of triazinanes with 1,2-epoxypropane.

(**2a**) **compound ^{1}H NMR (300 MHz, DMSO-d$_6$, δ):** d (mixture of two diastereoisomers) = 0.96 (t, 3H, CH_3), 1.48 (d, J = 8.5 Hz, 2H, CH_2), 1.78 (t, J = 12.25 Hz, 1 H, NH), 2.27 (s, 3H, CH_3), 2.28 (t, J = 8.5 Hz, 1H, NH), 3.45 (d, 1H, CH), 3.47, 3.72, (d, J = 12.25 Hz, 2H, CH_2), 4.81 (d, 1H, OH), 5.04 (d, 2H, 2CH–triazine), 6.9 (m, 8H, CH–Ar).

^{13}C NMR (75 MHz, DMSO-d$_6$): d (mixture of two diastereoisomers) = 7.6 (CH_3-Alk), 24.3 (CH_3–Ar), 28.6 (-CH_2-), 33 (CH_3–N-), 56.5 (-CH_2-), 71.2 [-CH (OH)], 79.3 (-CH–triazinane), 81.7 (-CH–triazinane), 128.7, 135.3, 136.9 (-CH–Ar), 177.3 (C=S).

(**2b**) **compound - ^{1}H NMR (300 MHz, DMSO-d$_6$, δ):** d (mixture of two diastereoisomers) = 1.21 (t, 3H, CH_3), 2.19 (s, 3 H, CH_3), 2.02 (t, J = 11.5 Hz, 1H, NH), 2.27 s (3H, CH_3N), 3.47 3.72, (d, J = 11.5 Hz, 2H, CH_2), 3.63 [d, 1H, CH (OH)], 4.81 (d, 1H, OH), 5.01 (s, 1H, CH), 6.9 (m, 8H, CH–Ar).

^{13}C NMR (75 MHz, DMSO-d_6): d (single diastereoisomer, *trans*) = 23 (-CH_3-Alk), 24.3 (CH_3–Ar), 33 (CH_3–N-), 59 (-CH_2-), 66.2 [-CH (OH)], 79.3 (-CH–triazinane), 81.7 (-CH–triazinane), 128.7, 135.3, 136.9 (-CH–Ar), 177.3 (C=S).

2.4.10 | 1,3-*bis*(4-Hydroxybutan-2-yl)-5-methyl-4,6-*bis*(*p*-tolyl)-1,3,5-triazinane-2-thione (2c)

5-Methyl-4,6-di(*p*-tolyl)-1,3,5-triazinane-2-thion (1b) (0.01 mol) was dissolved in 5–10 ml acetyl acetone and ethyl alcohol, which were the reactive chemicals, in a 2:1 molar ratio, and added to the solution slowly. 4-Chlor-butanol-1 was added and mixed for 10–15 min. After that, triethylamine catalyst was added and mixed. The solution was mixed at 70–78°C temperature for 1–3 h. After the completion of the reaction, the mixture was cooled, purified by means of re-crystallization with ethanol and dried.

^{1}H NMR (300 MHz, DMSO-d_6, δ): d (single diastereoisomer, *trans*) = 1.10 (t, 3H, CH_3), 1.56 (d, 2H, CH_2), 2.19 s (6H, 2CH_3–Ar), 2.27 (s, 3H, CH_3N), 2.29 (t, J = 12.25 Hz, 1 H, NH), 2.79 (d, J = 12.25 Hz, 2H, CH_2), 3.53 (d,1H, CH), 4.78 m (1H, OH), 6.94 m (8H, CH–Ar).

^{13}C NMR (75 MHz, DMSO-d_6): d (single diastereoisomer, *trans*) = 19 (-CH_3-Alk), 24.3 (CH_3–Ar), 33 (CH_3–N-), 38.8 (-CH_2-), 50.8 (-CH–CH_3), 58.3 (-CH_2–OH), 78.9 (-CH–triazinane), 79.3 (-CH–triazinane), 128.7, 135.9, 136.9 (-CH–Ar), 176.9 (C=S).

2.4.11 | 1,3-*bis*(3-Chloro-2-hydroxypropyl)-5-methyl-4,6-*bis*(*p*-tolyl)-1,3,5-triazinane-2-thione (2d)

5-Methyl-4,6-di(*p*-tolyl)-1,3,5-triazinane-2-thion (1b) (0.01 mol) was dissolved in a 2:1 ratio of acetylacetone and ethyl alcohol (10:5 ml). Then, epichlorohydrin (0.26 ml, 3.3 mmol) was added drop by drop. After dissolving in the stirrer for 25 min, 0.03 g $AlCl_3$ catalyst was added and mixed by heating at 65–70°C. After determining the full completion of reaction, the solution was evaporated and cleansed in ethyl alcohol solution.

^{1}H NMR (300 MHz, DMSO-d_6, δ): d (mixture of two diastereoisomers) = 2.19 s (3 H, CH_3), 2.27 s (3H, CH_3N), 2.45 (t, J = 11.75 Hz, 1 H, NH), 3.40, 3.65, (d, J = 11.75 Hz, 2H, CH_2), 3.47, 3.72 (d, J = 8.5 Hz, 2H, CH_2), 3.77 [d 1H, CH (OH)], 5.01 (s, J = 8.5 Hz, 1H, CH), 4.81 (m, 1H, OH), 6.9 (m, 8H, CH–Ar).

^{13}C NMR (75 MHz, DMSO-d_6): d (mixture of two diastereoisomers) = 24.3 (CH_3–Ph), 33 (CH_3–N-), 49.5 (-CH_2Cl), 53.9 (-CH_2–N-), 74.1 [-CH (OH)], 79.3 (-CH–triazinane), 81.7 (-CH–triazinane), 128.7, 135.9, 136.9 (-CH–Ar), 177.3 (C=S).

2.5 | Biochemical studies

2.5.1 | hCA Isoenzyme purification and inhibition studies

For investigating of inhibitory effects of novel *N*-substituted triazinane-2-thiones derivatives (**1a–g** and **2a–d**) on hCA isoforms, both hCA isoforms from human erythrocytes were purified via a simple single-step method using Sepharose-4B-L-Tyrosine-sulphanilamide affinity gel chromatography.[30,31] For this purpose, the human erythrocyte samples were centrifuged at 13,000 rpm for 25 min.[32] Then, the solution was filtered to remove the precipitate. Both hCA isoenzymes were isolated from the serum, the pH of which was adjusted to 8.7 by adding solid Tris.[33] Affinity column was equilibrated by buffer solution (25 mM Tris–HCl–/0.1 M Na_2SO_4) at pH 8.7. The serum was loaded on the affinity gel and washed with buffer solution (25 mM Tris–HCl/22 mM Na_2SO_4 at pH 8.7). The hCA I isoenzyme was eluted by buffer solution (1.0 M NaCl/0.25 M sodium phosphate at pH 6.3). On the other hand, hCA II isoenzyme was eluted by another buffer solution (0.1 M sodium acetate/0.5 M $NaClO_4$ at pH 5.6). Both isoenzymes were taken from the column in fractions of 2 ml.[34] All work was carried out at 4°C. The hCA isoenzymes activity were measured by following the change in specific absorbance (348 nm) of *p*-nitrophenylacetate to *p*-nitrophenolate ion over a period of 3 min at room temperature (25°C) using a spectrophotometer (Thermo Scientific, UV–vis spectrophotometer) according to the method of Verpoorte et al.[35] There was 0.4 ml of 0.05 M Tris–SO_4 buffer (pH 7.4), 3 ml of 3 mM *p*-nitrophenylacetate, 0.2 ml of H_2O and 0.1 ml of enzyme solution in the test tube content of this reaction.[36] Esterase activity assays were identified from a series of experiments at three different novel pyrazoles derivatives (**Py1–8**).

2.5.2 | AChE inhibition study

The inhibitory effects of novel *N*-substituted triazinane-2-thiones derivatives (**1a–g** and **2a–d**) on AChE activity were performed according to the spectrophotometric method of Ellman et al.[37] Acetylthiocholine iodide (AChI) substrate was utilized for the inhibition act and enzymatic reaction. 5,5′-Dithio-*bis*(2-nitro-benzoic) acid (DTNB) compound was utilized in this study for the

measurement of the AChE activity. Briefly, 750 μL of sample solution dissolved in deionized water at different concentrations with 100 μL of Tris/HCl buffer (1.0 M, pH 8.0) and 50 μL of AChE solution were mixed and incubated for 64 min at 21°C.[38,39] Then reaction was initiated by the addition of 50 μL of AChI. Then 50 μL of DTNB (0.5 mM) was added. The hydrolysis of these substrates was monitored spectrophotometrically by formation of the yellow 5-thio-2-nitrobenzoate anion as the result of the reaction of thiocholine with DTNB, released by enzymatic hydrolysis of AChI, with an absorption maximum at a wavelength of 412 nm.[40–45] For the computation of K_i values of these compounds, three diverse novel *N*-substituted triazinane-2-thiones derivatives (**1a–g** and **2a–d**) concentrations were utilized. One AChE enzyme unit is the amount of enzyme that hydrolyzes 1.0 mol of AChI to choline and acetate per minute at pH 8.0 at 37°C. Finally, the Lineweaver–Burk[46] curves were drawn.

2.5.3 | Measurement of α-glycosidase inhibitory activity

α-Glycosidase inhibitory efficacy of novel *N*-substituted triazinane-2-thiones derivatives (**1a–g** and **2a–d**) was performed using *p*-nitrophenyl-D-glycopyranoside (*p*-NPG) as the substrate, according to the procedure of Tao et al.[47] Samples were prepared by dissolving 10 mg in 10 ml (EtOH: H_2O). First, 100 μL of phosphate buffer was mixed with 30 μL of the enzyme solution in phosphate buffer (0.15 U/ml, pH 7.4) and 30–200 μL of the sample.[48] Multiple solutions in phosphate buffer were prepared in case of full enzyme inhibition. Then it was preincubated at 30°C for 10 min prior to adding the *p*-NPG for the initiation of the reaction. Also, 50 μL of *p*-NPG in phosphate buffer (5 mM, pH 7.4) after preincubation was added and again incubated at 37°C. The absorbances were spectrophotometrically measured at 405 nm.[49,50] The IC_{50} amount was calculated from activity (%) vs. plant concentration plots. Lineweaver–Burk graphs were used to determine V_{max} and other inhibition parameters. The K_i was calculated from these graphs.

3 | RESULTS AND DISCUSSION

3.1 | Chemistry

At the first stage, new cyclic compounds were synthesized on the basis of thiourea amines and triple-component condensation with salicylic aldehyde and their various transformations were investigated. Thus, 5-(1,5-diaminopentan-3-yl)-4,6-dihydrochloride is a result of the thiourea trifluorous acetic acid catalyst reaction in combination with benzaldehyde, salicylic aldehyde, anisilaldehyde and three-component condensation at a single stage with various amines, *bis* (2-hydroxyphenyl)-1,3,5-triazinane-2-thione (**1a**), 5-methyl-4,6-di(*p*-tolyl)-1,3,5-triazinane-2-thione (**1b**), 5-ethyl-4,6-*bis*(2-hydroxyphenyl)-1,3,5-triazinane-2-thione (**1c**), 4,6-diphenyl-1,3,5-triazinane-2-thione (**1d**), 5-ethyl-4,6-di(*p*-tolyl)-1,3,5-triazinane-2-thione (**1e**), 5-methyl-4,-6-*bis*(4-methoxyphenyl)-1,3,5-triazinane-2-thione (**1f**) and 60–70% yield-effective synthesis of 5-ethyl-4,-6-*bis*(4-methoxyphenyl)-1,3,5-triazinane-2-thione (**1 g**) (Scheme 1).

At the next stage, reactions of triazinanes with nucleophilic reagents were investigated. New compounds (**2a–d**) which are not known in the literature were synthesized from interaction of 5-methyl-4,6-*bis*(*p*-tolyl)-1,3,5-triazinane-2-thione (**1b**) with 1,2-epoxybutane, 1,2-epoxypropane, 3-chlor-butanol-1 and 1,2-epoxy-3-chloropropane as nucleophilic reagents (Scheme 2). The physical–chemical constraints and output of synthesized compounds (**1a–g** and **2a–d**) are shown in Table 1.

3.2 | Computational investigation

We computed a model reaction of Scheme 1 which yields selectively 4,6-diphenyl-1,3,5-triazinane-2-thione (**1d**). The computations were performed by using Discrete fourier transform (DFT) with the B3LYP functional and 6-31G*[51] basis sets for H, C, N, F and O. The 6–31++G(d,p) basis was used for sulfur and chlorine in the catalyst (CX_3COOH) according to recent recommendations.[52] Other (e.g. WB97XD, M06 L) along with the

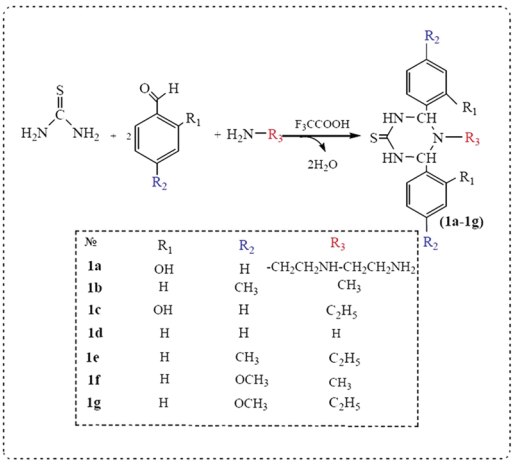

№	R_1	R_2	R_3
1a	OH	H	-CH2CH2NH-CH2CH2NH2
1b	H	CH3	CH3
1c	OH	H	C2H5
1d	H	H	H
1e	H	CH3	C2H5
1f	H	OCH3	CH3
1g	H	OCH3	C2H5

SCHEME 1 Derivatives of triazinanethione (**1a–1g**)

SCHEME 2 Derivatives of triazinane-thione (**2a–2d**)

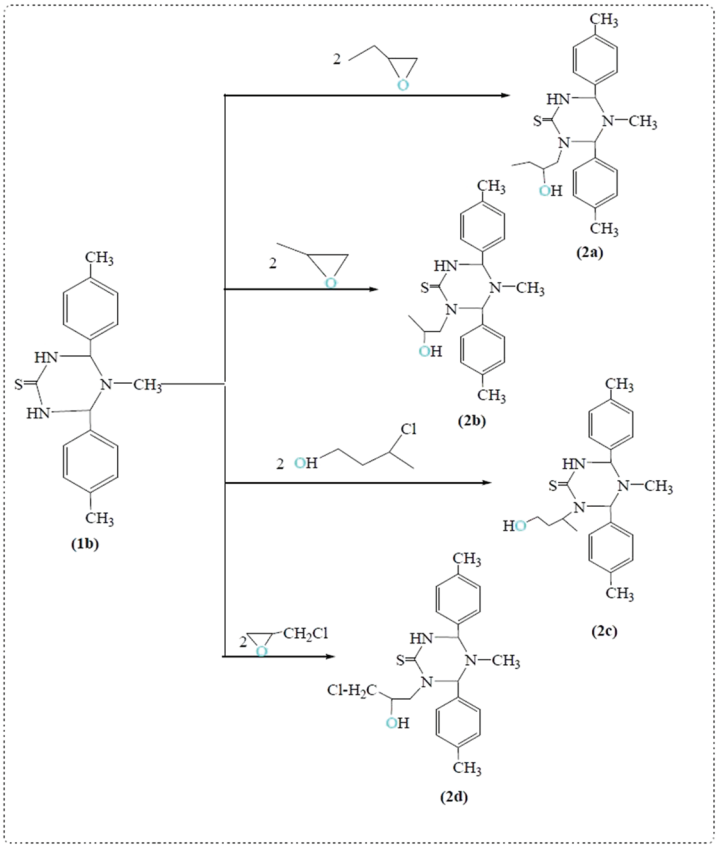

same basis sets was tested for the optimization of intermediate and transition state structures. In particular, sulfur-containing structures could not be optimized. Calculations show that B3LYP is better at describing delocalization in the thiourea structure. The Gaussian 09 package was used for all calculations.[53] The reaction

TABLE 1 Physico-chemical characteristics of derivatives of triazinane-thione

Number	Compounds	$T_{m.p.}$ (°C)	Brutto Formula	Found/calculated (%) C	H	N	S	Yield (%)
1a	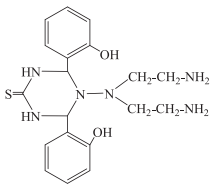	175–176	$C_{19}H_{26}O_2N_5S$	58.74/58.76	6.68/6.70	18.04/18.06	8.25/8.26	81
1b	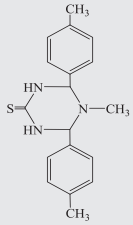	166–168	$C_{18}H_{21}N_3S$	69.42/69.45	6.73/6.75	10.82/10.84	10.29/10.27	76

(Continues)

TABLE 1 (Continued)

Number	Compounds	$T_{m.p.}$ (°C)	Brutto Formula	Found/calculated (%) C	H	N	S	Yield (%)
1c	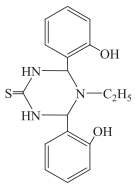	177	$C_{17}H_{19}O_2N_3S$	61.98/62.01	5.75/5.78	12.76/12.77	9.73/9.75	89
1d	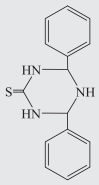	112	$C_{15}H_{15}N_3S$	66.89/66.92	5.53/5.58	15.48/15.51	11.75/11.90	85
1e	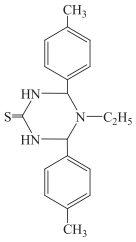	192–194	$C_{19}H_{23}N_3S$	70.12/70.15	7.04/7.08	12.92/12.93	9.85/9.86	89
1f	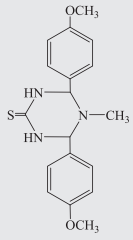	178	$C_{18}H_{21}O_2N_3S$	62.94/62.97	6.09/6.12	12.24/12.26	9.33/9.34	77
1 g	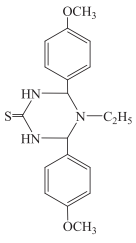	179–181	$C_{19}H_{23}O_2N_3S$	63.85/63.86	6.41/6.44	11.76/11.78	8.96/8.99	70

(Continues)

TABLE 1 (Continued)

Number	Compounds	$T_{m.p.}$ (°C)	Brutto Formula	Found/calculated (%) C	H	N	S	Yield (%)
2a	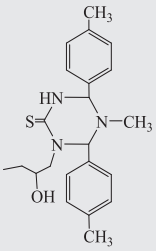	205	$C_{22}H_{29}ON_3S$	68.91/68.93	7.53/7.57	10.97/10.99	8.35/8.37	65
2b	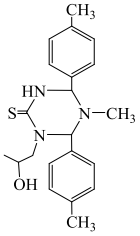	197	$C_{21}H_{27}ON_3S$	68.24/68.29	7.29/7.32	11.38/11.41	8.67/8.69	86
2c	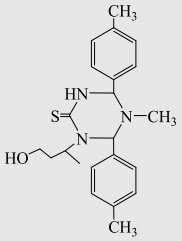	200–202	$C_{22}H_{29}ON_3S$	68.88/68.93	7.27/7.32	10.97/10.98	8.35/8.36	68
2d	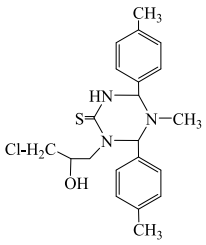	195–196	$C_{21}H_{26}ON_3SCl$	62.42/62.45	6.39/6.44	10.01/10.03	7.63/7.65	64

path was calculated both for experimental reaction conditions (1 atm, 313.15 K), and for 1 atm, 373 K to see the effect of elevated temperature on energy barriers. The solvent effect was calculated with a self-consistent reaction field continuum solvation model (with a dielectric constant for water). Optimized Cartesian coordinates, total energies, Gibbs energies and enthalpies of all structures were calculated.

The over-the-counter (OTC) synthesis mechanism of 4,6-diphenyl-1,3,5-triazinane-2-thione (**1d**) was initiated with ammonia benzaldehyde interaction (Scheme 3). We previously investigated and scrutinized theoretically the interaction of small molecules as a starting point of a reaction in multicomponent synthesis.[54] The amine group of this intermediate reacted further with additional benzaldehyde molecule. After the dihydroxylation step

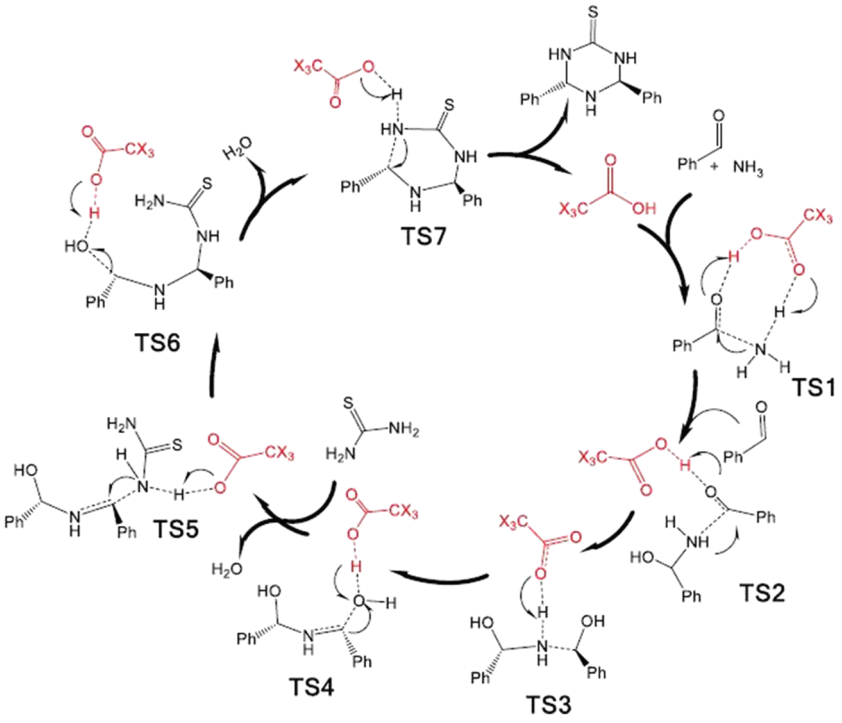

SCHEME 3 Quantum chemical calculation based mechanism of CX_3COOH catalyzed OTC condensation reaction (**1d**)

(**TS4**) the thiourea amine group attacked the olefinic carbon of the intermediate (see **TS5**). Further dihydroxylation (**TS6**) and proton abstraction (**TS7**) resulted in the product (4,6-diphenyl-1,3,5-triazinane-2-thione) formation. We calculated the reaction (Scheme 1) cycle three times, changing the hydrogen atoms of the methyl group in AA with fluorine and chlorine atoms. The potential energy surface diagram in Figure 1 includes whole three cycles of the OTC mechanism with AA, TFA, and TCA catalysts. The computation shows that there is not a major difference in energy barriers (see energy span for the routes) for AA and TFA catalyzed routes (grey and blue in Figure 1). Surprisingly, TCA minimizes energy barriers considerably compared with the AA and TFA.

Structural analysis of the initial three transition states of Figure 1 clearly shows how halogen atoms affect energy barriers. As seen from the **F-TS1** and **Cl-TS1**, the catalyst O–H bonds (1.08 and 1.10 Å) are elongated compared with the AA (1.04 Å) case (**H-TS1**). Replacement of the methyl hydrogen atoms with halogen atoms in AA facilitates proton transfer via the elongated bonds to the oxygen of the benzaldehyde carbonyl and as a result decreases the energy barrier by

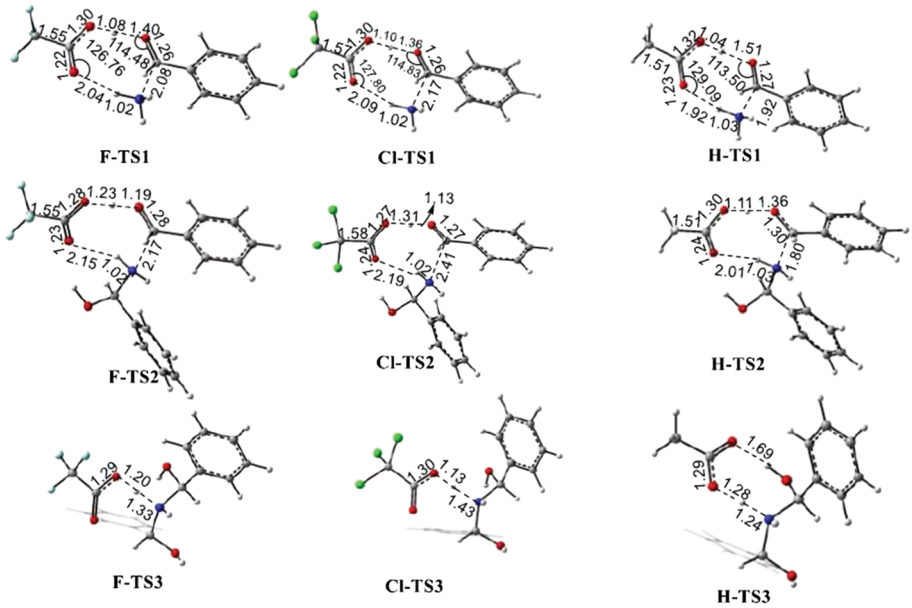

FIGURE 2 The optimized structures of **F-TS1**, **F-TS2**, **F-TS3**, **Cl-TS1**, **Cl-TS2**, **Cl-TS3**, **H-TS1**, **H-TS2** and **H-TS3** with important bond lengths (given in Å) and angles (deg). Phenyl groups are omitted for clarity

about 6 kcal/mol. The benzaldehyde interaction with azanediyl*bis* (phenylmethanol; **F-INT2, Cl-INT2,** and **H-INT2**) requires higher activation energy (**F-TS2** 25.2 kcal/mol and **Cl-TS2** 27.2 kcal/mol) in the case of halogenated acetic acids for **INT2TS2**. AA acts as a reasonable catalyst, here rendering proton transfer to the carbonyl oxygen via 23.4 kcal/mol energy barrier. AA is also a superior catalyst for the dialkylammonium (-NH_2^+-, **H-INT4**) deprotonation (**H-TS3**, $\Delta G = 0.1$ kcal/mol). It can be rationalized with the AA binding to the structure (see Figure 2, **H-TS3**) via hydrogen bonding (1.68 Å) between the hydroxyl and the acetic acid carbonyl group. This kind of design of the structure is not seen in analogous halogen-bearing transition states (**F-TS3** and **Cl-TS3**). In these transition states, the carbonyl of the catalyst and the hydroxyl cannot be prone to hydrogen bonding because of the low electron density (electron density flows toward halogen atoms) on the carbonyl oxygen. At the next stage, one of the hydroxyl groups attached to the benzylic carbons was removed via dehydration (**F-, Cl-** and **H-TS4**). Catalytic performance of the AA declines at the next step, dehydration energy barrier (**H-TS4**), was calculated to be 10.4 kcal/mol, which is 7.7 kcal **F-TS4,** and 7.3 kcal higher than the **Cl-TS4** energy barrier. The thiourea (**INT6TS5**) and benzaldehyde (**INT2TS2**) additions to the cycle were calculated to have the highest energy barriers, and can be accepted as rate-limiting steps for all three cycles (grey, orange and blue).

The activation energy of TFA-catalyzed thiourea addition (**F-TS5**, 26.8 kcal/mol) was greater than that for TCA (**Cl-TS**, 25.9 kcal/mol) and AA (**H-TS5**, 24 kcal/mol). The smallest activation energy was seen with the **H-TS5** structure. As seen from Figure 3 the AA carbonyl oxygen binds to proton (-NH-) of the intermediate via hydrogen bonding (1.88 Å), which serves as a supporter for the acid for easy proton abstraction from the thiourea amine group. The last hydroxyl abstraction generates an intermediate for the ring closure. The hydroxyl abstraction occurs via the smaller energy barriers (almost barrierless) for TCA (**Cl-TS6**) and TFA (**F-TS6**) acid-catalyzed routes. This route was calculated to be 12 kcal/mol energetic in case of AA, despite structural orientations (e.g. bond lengths, angles and hydrogen bonding) being quite similar to those in the halogenated catalysts case. The nucleophilic attack from the thiourea amine group to the sp^2 hybridized carbon (hydroxyl group from the carbon at the previous step) yielded the product formation via ring closure (see Figure 4).

TS7 in the three cases (grey, blue, and orange) were concerted transition states because of proton abstraction from the thiourea amine group and the ring closure occurring at the same time. The activation energies were 22.2, 20.4 and 19.3 kcal/mol, respectively, for **F-TS7**, **H-TS7** and **Cl-TS7**. Overall reaction was calculated to be 33.4 kcal/mol endergonic reaching the product as a *trans* conformer.

At the reference, solvent-induced conversion of the *cis* conformer to *trans* in a polar solvent and the stability of the *trans* conformer were studied by XRD and NMR analysis. Our calculations are in good agreement with the experimental observations showing that the *trans* conformer (4,6-diphenyl-1,3,5-triazinane-2-thione) is stable in the water medium. The *cis* conformer could

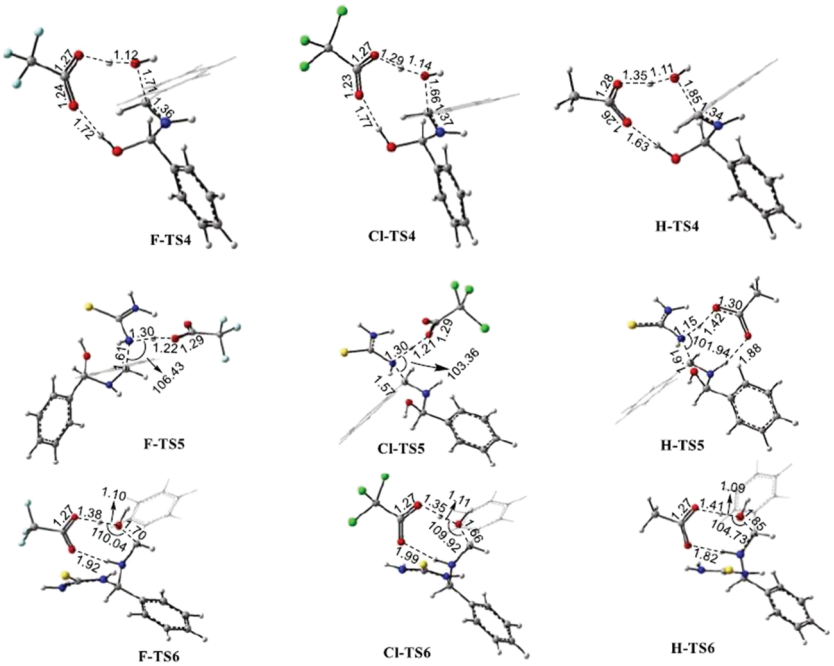

FIGURE 3 The optimized structures of **F-TS4**, **F-TS5**, **F-TS6**, **Cl-TS4**, **Cl-TS5**, **Cl-TS6**, **H-TS4**, **H-TS5** and **H-TS6** with important bond lengths (given in Å) and angles (deg). Phenyl groups are omitted for clarity

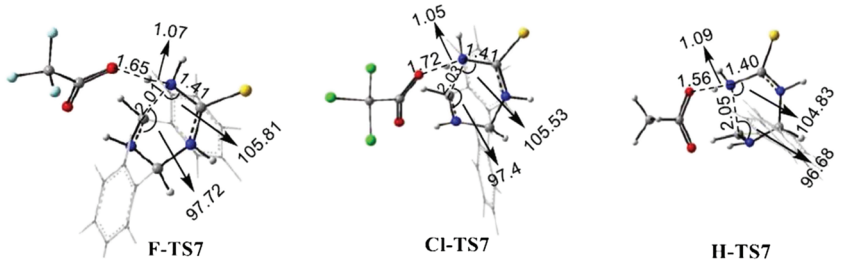

FIGURE 4 The optimized structures of **F-TS7**, **Cl-TS7**, and **H-TS7** with important bond lengths (given in Å) and angles (deg). Phenyl groups are omitted for clarity

not be allocated for the **TS7**. Moreover, the *trans* arrangement of the product phenyl groups started from **TS3** and further optimized transition states and intermediates.

3.3 | Pharmacological results

The cytosolic hCA I, and II isoforms are ubiquitous and both can be used for treatment of diseases (e.g. as anti-glaucoma or diuretics factors) and off-targets.[55] Also, the membrane-associated hCA IV isoenzyme is a drug used for multiple pathologies, like retinitis pigmentosa, glaucoma (together with hCA II and XII), rheumatoid arthritis and stroke.[56] Presently, there are 22 clinically utilized CA inhibitor compounds, but all of them are show little or no isoenzyme specificity.[57] Because if this, there is a need to develop CA inhibitor compounds that are isoenzymes selective, for instance, the targeted inhibition action of CA IX isoform can be used for anticancer chemotherapy.[58] The design of CA isoform-specific inhibitor compounds is challenging owing to the high sequence similarity within the active sites and structural homology of the active CA isoenzymes. Additionally, we report the inhibition effect of novel *N*-substituted triazinane-2-thiones derivatives (**1a–g** and **2a–d**) on two catalytically active isoforms, hCA I and II, as well as against AChE and α-glycosidase enzymes. The enzymes inhibition activity data of novel *N*-substituted triazinane-2-thiones derivatives (**1a–g** and **2a–d**) reported here are shown in Table 2, and the following comments can be drawn from these data.

The results presented in Table 2 indicate that novel *N*-substituted triazinane-2-thiones derivatives (**1a–g** and **2a–d**) had an effective inhibition profile against slow cytosolic hCA I isoform. The hCA I isoform was inhibited by these compounds at low nanomolar levels, the K_i of which differed between 13.44 ± 4.39 and 74.98 ± 6.25 nM. On the other hand, acetazolamide, considered a broad-specificity CA inhibitor owing to its widespread inhibition of CAs, showed a K_i value of 120.36 ± 15.85 nM against hCA I isoenzyme. Among the inhibitors, 5-methyl-4,6-*bis*(*p*-tolyl)-1,3,5-triazinane-2-thione (**1b**) and 5-ethyl-4,6-*bis*(*p*-tolyl)-1,3,5-triazinane-2-thione (**1e**) were obtained as excellent hCA I inhibitors with values of K_i of 13.44 ± 4.39 and 30.36 ± 3.45 nM, respectively. The hCA I inhibition effects of all novel *N*-substituted triazinane-2-thiones derivatives (**1a–g** and **2a–d**) were found to be greater than that of acetazolamide, which was a clinically standard CA inhibitor.

Against the physiologically dominant isoform hCA II, novel *N*-substituted triazinane-2-thione derivatives (**1a–g** and **2a–d**) demonstrated values of K_i varying from 10.41 ± 4.8 to 72.6 ± 17.66 nM (Table 2). These compounds had high inhibition effects toward hCA II. On the other hand, the standard compound acetazolamide showed K_i of 106.73 ± 20.73 nM against hCA II. 1,3-*bis*(2-Hydroxypropyl)-5-methyl-4,6-*bis*(*p*-tolyl)-1,3,5-triazinane-2-thione (**2b**) and 4,6-diphenyl-1,3,5-triazinane-2-thione (**1d**) showed the most inhibition effect with K_i values of 10.41 ± 4.8 and 13.66 ± 2.36 nM, respectively.

Recently, many synthetic or natural compounds and their derivatives were discovered as a novel potential therapies for the treatment of AD.[59] Followed by these evaluations, classes of synthetic and natural products derivatives were synthesized and investigated for AChE enzyme inhibitory activity in our laboratory.[60] In our study, novel *N*-substituted triazinane-2-thione derivatives (**1a–g** and **2a–d**) were investigated for their ability to inhibit AChE, which was the primary ChE in the body. According to our data, inhibitory results of these molecules revealed a significant elevation in the case of AChE. Considering the results, all molecules expressed appreciably higher inhibition activity. All of these derivatives had significantly higher AChE inhibitory activity than standard AChE inhibitors such as tacrine. The K_i values of these compounds and standard compound (tacrine) are summarized in Table 2. As can be seen from the results obtained, these compounds effectively inhibited AChE, with K_i values in the range of 36.82 ± 9.95 to 108.48 ± 1.17 nM. However, all of these compounds had similar inhibition profiles. The most active 5-ethyl-4,6-*bis*(2-hydroxyphenyl)-1,3,5-triazinane-2-thione (**1c**), 5-ethyl-4,6-*bis*(*p*-tolyl)-1,3,5-triazinane-2-thione (**1e**) and 5-methyl-4,6-*bis*(4-methoxyphenyl)-

TABLE 2 The enzyme inhibition results of novel *N*-substituted triazinane-2-thiones derivatives (**1a–g** and **2a–d**) against cytosolic carbonic anhydrase I and II isoforms (hCA I and II), acetylcholinesterase (AChE) and α-glycosidase enzymes

	IC_{50} (nM)								K_i (nM)			
Compounds	**hCA I**	r^2	**hCA II**	r^2	**AChE**	r^2	**α-Gly**	r^2	**hCA I**	**hCA II**	**AChE**	**α-Gly**
1a	22.94	0.9501	20.06	0.9541	145.74	0.9651	832.45	0.9743	53.84 ± 8.57	72.6 ± 17.66	98.40 ± 4.19	812.73 ± 92.18
1b	15.3	0.9721	14.57	0.9302	106.78	0.9433	1043.11	0.9811	13.44 ± 4.39	65.67 ± 11.22	80.43 ± 3.33	943.12 ± 109.33
1c	14.08	0.9923	13.54	0.9522	62.91	0.9533	803.18	0.9720	70.38 ± 14.64	49.91 ± 16.26	36.82 ± 9.95	835.82 ± 163.14
1d	11.49	0.9472	12.31	0.9322	86.87	0.9462	581.44	0.9614	73.32 ± 18.08	13.66 ± 2.36	68.16 ± 10.56	649.15 ± 88.81
1e	15.01	0.9524	14.29	0.9361	91.63	0.9664	613.73	0.9305	30.36 ± 3.45	59.13 ± 16.45	40.28 ± 9.70	624.62 ± 100.34
1f	13.94	0.9472	13.94	0.9472	77.20	0.9872	1083.20	0.9572	74.98 ± 6.25	59.87 ± 5.21	42.82 ± 9.72	1124.16 ± 205.14
1g	15.15	0.9662	13.07	0.9241	148.63	0.9764	1014.23	0.9683	49.65 ± 7.79	47.98 ± 4.96	95.41 ± 15.3	983.15 ± 184.04
2a	15.73	0.9702	14.86	0.9291	124.53	0.9833	748.23	0.9835	43.5 ± 11.49	56.2 ± 8.59	74.5 ± 7.10	803.10 ± 191.28
2b	16.31	0.9303	18.04	0.9453	155.84	0.9622	703.18	0.9715	65.74 ± 12.51	10.41 ± 4.8	108.48 ± 1.17	745.91 ± 73.92
2c	19.05	0.9742	16.02	0.9534	82.54	0.9653	783.53	0.9932	71.25 ± 17.84	65.43 ± 3.36	96.68 ± 20.09	738.27 ± 205.17
2d	20.92	0.9611	16.45	0.9322	141.70	0.9901	968.51	0.9716	38.15 ± 5.09	36.55 ± 10.95	83.48 ± 8.6	1015 ± 148.14
AZA[a]	148.23	0.9883	131.63	0.9823	—	—	—	—	120.36 ± 15.85	106.73 ± 20.73	—	—
TAC[b]	—	—	—	—	163.73	0.9912	—	—	—	—	129.63 ± 11.65	—
ACR[c]	—	—	—	—	—	—	22800	—	—	—	—	12600 ± 780

[a]AZA (acetazolamide) was used as a positive control for hCA I and II.
[b]TAC (tacrine) was used as a positive control for AChE and butyrylcholinesterase enzymes.
[c]ACR (acarbose) was used as a positive control for α-glycosidase enzyme. This has been taken from references.[67,68]

1,3,5-triazinane-2-thione (**1d**) showed K_i values of 36.82 ± 9.95, 40.28 ± 9.70 and 42.82 ± 9.72 nM, respectively. Three out of the four drug compounds newly approved for the therapy of AD are based on the inhibition of AChE enzyme; hence, their usefulness is as yet limited since the long-term (for instance, >6 months) efficacy and safety are not entirely clear. Thus, the development of efficient bioanalytical procedures for the analysis of AChEIs in biological samples is important in assessing the pharmacokinetics and bioavailability of these drugs as well as related compounds, metabolites and degradation products.

Postprandial glucose rates can be adjusted via α-glycosidase inhibitor compounds. Inhibition of this enzyme delays and in some cases halts carbohydrate digestion, thus prolonging overall carbohydrate digestion time, causing a reduction in the rate of glucose absorption and accordingly decreasing postprandial plasma glucose rise.[61] Currently, α-glycosidase inhibitor compounds like miglitol, acarbose and voglibose are oral blood glucose-lowering drugs that are generally utilized.[62] They are also the only drug class that does not pose a pathophysiological issue in type 2 diabetes melitis.[63] They reduce postprandial hyperglycemia without inducing insulin secretion; these compounds do not induce hypoglycemia and have a good safety profile, although gastrointestinal adverse effects may limit long-term compliance with therapy.[64] The research for the new group of factors from natural resources, especially from traditional medicines, has become an attractive approach for the treatment of postprandial hyperglycemia.[65] For the α-glycosidase enzyme, the novel *N*-substituted triazinane-2-thiones derivatives (**1a–g** and **2a–d**) had IC_{50} values in the range of 581.44–1083.20 nM and K_i values in the range of 624.62 ± 100.34–1124.16 ± 205.14 nM (Table 2 and Figure 5). The results clearly recorded that all these derivatives (**1a–g** and **2a–d**) demonstrated efficient α-glycosidase inhibitory effects compared with acarbose (IC_{50}: 22.8 μM)[66,67] as a standard α-glycosidase inhibitor. Indeed, the most effective K_i values were obtained by 5-ethyl-4,6-*bis*(*p*-tolyl)-1,3,5-triazinane-2-thione (**1e**) and 4,6-diphenyl-1,3,5-triazinane-2-thione (**1d**), with K_i values of 624.62 ± 100.34 and 649.15 ± 88.81 nM, respectively.

Animal research has revealed that glucose may improve memory through a facilitation of acetylcholine synthesis and release in the brain. This glucose-related memory improvement has prompted research in elderly humans. These studies have shown that the memory-improving action of glucose depends on each individual's blood glucose regulation. Based on these data, researchers have evaluated the effect of glucose on memory in patients with AD. DM contributes to cognitive impairment in the elderly, and constitutes a risk factor for dementia, possibly including Alzheimer's disease. The development of effective synthetic α-glycosidase inhibitors may prove important for antidiabetic chemotherapy and treatments for other related disorders. These compounds are also excellent carbonic anhydrase inhibitors, making them interesting antiglaucoma drug candidates.

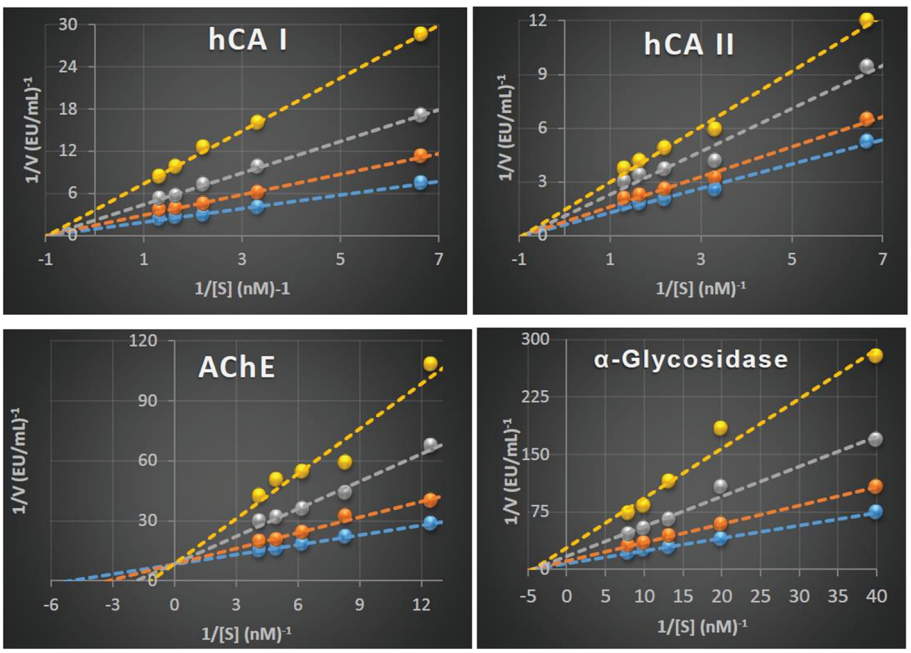

FIGURE 5 Determination of Lineweaver–Burk graphs for excellent inhibitors of hCA I (**1b**), hCA II (**1b**), acetylcholinesterase (AChE) (**1c**) and α-glycosidase (**1d**) enzymes

4 | CONCLUSIONS

Novel *N*-substituted triazinane-2-thiones derivatives (**1a–g** and **2a–d**) were used in the present paper and also recorded efficient inhibition profiles against AChE, hCA I and II, and α-glycosidase enzymes. In this paper, nanomolar levels of IC_{50} values were obtained for all derivatives on these metabolic enzymes. Thus, these compounds can be selective inhibitors of α-glycosidase and AChE enzymes as anticholinergic and antidiabetic drugs potentials.

CONFLICT OF INTEREST STATEMENT

The authors declare that there are no conflicts of interest.

ORCID

Parham Taslimi https://orcid.org/0000-0002-3171-0633

REFERENCES

[1] B. Kaboudin, T. Ghasemi, T. Yokomatsu, *Synthesis* **2009**, 3089.
[2] P. Taslimi, I. Gulcin, B. Ozgeris, S. Goksu, F. Tumer, S. H. Alwasel, C. T. Supuran, *J. Enzyme Inhib. Med. Chem.* **2016**, *31*, 152.
[3] H. İ. Gül, K. Kucukoglu, C. Yamali, S. Bilginer, H. Yuca, İ. Ozturk, P. Taslimi, I. Gulcin, C. T. Supuran, *J. Enzyme Inhib. Med. Chem.* **2016**, *31*, 568.
[4] P. Taslimi, I. Gulcin, N. Öztaşkın, Y. Çetinkaya, S. GÖksu, S. H. Alwasel, C. T. Supuran, *J. Enzyme Inhib. Med. Chem.* **2016**, *31*, 603.
[5] D. Ozmen Ozgun, C. Yamali, H. İ. Gül, P. Taslimi, I. Gulcin, T. Yanik, C. T. Supuran, *J. Enzyme Inhib. Med. Chem.* **2016**, *31*, 1498.
[6] A. Sujayev, E. Garibov, P. Taslimi, I. Gulcin, S. Gojayeva, V. Farzaliyev, S. H. Alwasel, C. T. Supuran, *J. Enzyme Inhib. Med. Chem.* **2016**, *31*, 1531.
[7] H. İ. Gül, M. Tuğrak, H. Sakagami, P. Taslimi, I. Gulcin, C. T. Supuran, *J. Enzyme Inhib. Med. Chem.* **2016**, *31*, 1619.
[8] H. Genç, R. Kalin, Z. Köksal, N. Sadeghian, U. M. Kocyigit, M. Zengin, I. Gulcin, H. Özdemir, *Int. J. Mol. Sci.* **2016**, *17*, 1736.
[9] B. Turan, K. Sendil, E. Sengul, M. S. Gultekin, P. Taslimi, I. Gulcin, C. T. Supuran, *J. Enzyme Inhib. Med. Chem.* **2016**, *31*, 79.
[10] F. Özbey, P. Taslimi, I. Gulcin, A. Maraş, S. Goksu, C. T. Supuran, *J. Enzyme Inhib. Med. Chem.* **2016**, *31*, 79.
[11] E. Garibov, P. Taslimi, A. Sujayev, Z. Bingöl, S. Çetinkaya, I. Gulcin, S. Beydemir, V. Farzaliyev, S. H. Alwasel, C. T. Supuran, *J. Enzyme Inhib. Med. Chem.* **2016**, *31*, 1.
[12] K. Aksu, B. Özgeris, P. Taslimi, A. Naderi, I. Gulcin, S. Goksu, *Arch. Pharm.* **2016**, *349*, 944.
[13] P. Taslimi, A. Sujayev, S. Mamedova, P. Kalın, I. Gulcin, N. Sadeghian, S. Beydemir, Ö. İ. Küfrevioglu, S. H. Alwasel, V. Farzaliyev, S. Mamedov, *J. Enzyme Inhib. Med. Chem.* **2017**, *32*, 137.
[14] H. I. Gul, A. Demirtas, G. Ucar, P. Taslimi, I. Gulcin, *Lett. Drug Des. Discov.* **2017**, *14*, 573.
[15] Ç. Bayrak, P. Taslimi, I. Gulcin, A. Menzek, *Bioorg. Chem.* **2017**, *72*, 359.
[16] A. Aktaş, P. Taslimi, I. Gulcin, Y. Gök, *Arch. Pharm.* **2017**, *350*, e1700045.
[17] P. Taslimi, A. Sujayev, E. Garibov, N. Nazarov, Z. Huyut, S. H. Alwasel, I. Gulcin, *J. Biochem. Mol. Toxicol.* **2017**, *31*, e21897.
[18] N. Öztaskın, P. Taslimi, A. Maras, S. Göksu, I. Gulcin, *Bioorg. Chem.* **2017**, *74*, 104.
[19] P. Taslimi, S. Osmanova, I. Gulcin, S. Sardarova, V. Farzaliyev, A. Sujayev, R. Kaya, F. Koc, S. Beydemir, S. H. Alwasel, O. I. Kufrevioglu, *J. Biochem. Mol. Toxicol.* **2017**, *31*, e21931.
[20] U. M. Koçyiğit, P. Taslimi, H. Gezegen, I. Gulcin, M. Ceylan, *J. Biochem. Mol. Toxicol.* **2017**, *31*, e21938.
[21] I. Gulcin, M. Abbasova, P. Taslimi, Z. Huyut, L. Safarova, A. Sujayev, V. Farzaliyev, S. Beydemir, S. H. Alwasel, C. T. Supuran, *J. Enzyme Inhib. Med. Chem.* **2017**, 321174.
[22] T. Dastan, U. M. Kocyigit, S. D. Dastan, P. Canturk Kiliçkaya, P. Taslimi, Ç. Özge, M. Koparir, *J. Biochem. Mol. Toxicol.* **2017**, *31*, e21971.
[23] U. M. Kocyigit, A. Taşkiran, P. Taslimi, A. Yokuş, Y. Temel, I. Gulcin, *J. Biochem. Mol. Toxicol.* **2017**, *31*, e21972.
[24] Y. Budak, U. M. Kocyigit, M. B. Gürdere, K. Özcan, P. Taslimi, I. Gulcin, M. Ceylan, *Synth. Commun.* **2017**, *47*, 2313.
[25] L. Zhang, S. Hogan, J. R. Li, S. Sun, C. Canning, S. J. Zheng, K. Q. Zhou, *Food Chem.* **2011**, *126*, 466.
[26] F. Hiroyuki, Y. Tomohide, O. Kazunori, *J. Nutr. Biochem.* **2001**, *12*, 351.
[27] T. Fujisawa, H. Ikegami, K. Inoue, Y. Kawabata, T. Ogihara, *Metabolism* **2005**, *54*, 387.
[28] S. Shobana, Y. N. Sreerama, N. G. Malleshi, *Food Chem.* **2009**, *115*, 1268.
[29] H. Wang, Y. J. Du, H. C. Song, *Food Chem.* **2010**, *123*, 6.
[30] U. M. Kocyigit, Y. Budak, F. Eligüzel, P. Taslimi, D. Kılıç, I. Gulcin, M. Ceylan, *Arch. Pharm.* **2017**, *350*, e1700198.
[31] Y. Demir, M. Işık, I. Gulcin, S. Beydemir, *J. Biochem. Mol. Toxicol.* **2017**, *31*, e21935.
[32] Z. Huyut, Ş. Beydemir, I. Gulcin, *J. Biochem. Mol. Toxicol.* **2017**, *31*, e21930.
[33] A. Akıncıoğlu, E. Kocaman, H. Akıncıoğlu, R. E. Salmas, S. Durdağı, I. Gulcin, C. T. Supuran, S. Göksu, *Bioorg. Chem.* **2017**, *74*, 238.
[34] L. Polat Köse, I. Gulcin, *Rec. Nat. Prod* **2017**, *11*, 558.
[35] J. A. Verpoorte, S. Mehta, J. T. Edsall, *J. Biol. Chem.* **1967**, *242*, 4221.
[36] K. Oktay, L. Polat Kose, K. Sendil, M. S. Gultekin, I. Gulcin, *Med. Chem. Res.* **2017**, *26*, 1619.
[37] G. L. Ellman, K. D. Courtney, V. Andres, R. M. Featherston, *Biochem. Pharmacol.* **1961**, *7*, 88.
[38] U. M. Koçyiğit, S. D. Daştan, P. Taslimi, T. Daştan, I. Gulcin, *J. Biochem. Mol. Toxicol.* **2018**, *32*, e22000.
[39] N. Bulut, U. M. Koçyiğit, I. H. Gecibesler, T. Dastan, H. Karci, P. Taslimi, S. Durna Dastan, I. Gulcin, A. Cetin, *J. Biochem. Mol. Toxicol.* **2018**, *32*, e22006.
[40] Y. Sarı, A. Aktaş, P. Taslimi, Y. Gök, C. Caglayan, I. Gulcin, *J. Biochem. Mol. Toxicol.* **2018**, *32*, e22009.

[41] U. M. Koçyiğit, Y. Budak, M. B. Gürdere, F. Ertürk, B. Yencilek, P. Taslimi, I. Gulcin, M. Ceylan, *Arch. Physiol. Biochem.* **2018**, *124*, 61.
[42] P. Taslimi, E. Sujayev, F. Turkan, E. Garibov, Z. Huyut, F. Farzaliyev, S. Mamedova, I. Gulcin, *J. Biochem. Mol. Toxicol.* **2018**, *32*, e22019.
[43] C. Yamali, H. İ. Gül, A. Ece, P. Taslimi, I. Gulcin, *Chem. Biol. Drug Des.* **2018**, *91*, 854.
[44] M. U. Koçyigit, P. Taslimi, F. Gurses, S. Soylu, S. Durna Dastan, I. Gulcin, *J. Biochem. Mol. Toxicol.* **2018**, *32*, e22031.
[45] F. Turkan, Z. Huyut, P. Taslimi, I. Gulcin, *J. Biochem. Mol. Toxicol.* **2018**, *32*, e22041.
[46] H. Lineweaver, D. Burk, *J. Am. Chem. Soc.* **1934**, *56*, 658.
[47] Y. Tao, Y. Zhang, Y. Cheng, Y. Wang, *Biomed. Chromatogr.* **2013**, *27*, 148.
[48] S. Burmaoglu, A. O. Yilmaz, P. Taslimi, O. Algul, D. Kılıç, I. Gulcin, *Arch. Pharm.* **2018**, *351*, e1700314.
[49] P. Taslimi, C. Caglayan, İ. GulÇin, *J. Biochem. Mol. Toxicol.* **2017**, *31*, e21995.
[50] P. Taslimi, H. Akıncıoğlu, I. Gulcin, *J. Biochem. Mol. Toxicol.* **2017**, *31*, e21973.
[51] W. J. Hehre, R. Ditchfield, J. A. Pople, *J. Chem. Phys.* **1972**, *56*, 2257.
[52] V. V. Chagovets, M. V. Kosevich, S. G. Stepanian, O. A. Boryak, V. S. Shelkovsky, V. V. Orlov, V. S. Leontiev, V. A. Pokrovskiy, L. Adamowicz, V. A. Karachevtsev, *J. Phys. Chem. C* **2012**, *116*, 20579.
[53] M. J. Frisch, G. W. Trucks, H. B. Schlegel, D. J. Fox, *Gaussian 09, Revision D.01*, Gaussian Inc., Wallingford, CT **2009**.
[54] Y. Abdullayev, A. Sudjaev, J. Autschbach, *J. Mol. Model.* **2019**, *25*(6), 173.
[55] C. Caglayan, I. Gulçin, *J. Biochem. Mol. Toxicol.* **2018**, *32*, e22010.
[56] F. Türkan, Z. Huyut, P. Taslimi, I. Gulçin, *Arch. Physiol. Biochem.* **2019**, *125*(1), 12. https://doi.org/10.1080/13813455.2018.1427766
[57] P. Taslimi, C. Çağlayan, F. Farzaliyev, F. Turkan, O. Nabiyev, A. Sujayev, F. Türkan, R. Kaya, İ. Gulçin, *J. Biochem. Mol. Toxicol.* **2018**, *32*, e22042.
[58] P. Taslimi, I. Gulçin, *J. Food Biochem.* **2018**, *42*(3), e12516.
[59] M. Rezai, Ç. Bayrak, P. Taslimi, İ. Gulçin, A. Menzek, *Turk. J. Chem.* **2018**, *42*(3), 808.
[60] N. Oztaşkın, Y. Çetinkaya, P. Taslimi, S. Göksu, I. Gulcin, *Bioorg. Chem.* **2015**, *60*, 49.
[61] T. M. C. Adachi, K. Sakurai, N. Shihara, K. Tsuda, K. Yasuda, *J. Endocrinol.* **2003**, *50*, 271.
[62] H. Laube, *Clin. Drug Investig.* **2002**, *22*, 141.
[63] X. Chen, Y. Zheng, Y. Shen, *Curr. Med. Chem.* **2006**, *13*, 109.
[64] M. Toeller, *Eur. J. Clin. Invest.* **1994**, *24*, 31.
[65] G. Slama, F. Elgrably, A. Sola, J. Mbemba, E. Larger, *Diabetes Metab.* **2006**, *32*, 187.
[66] M. Torres-Naranjo, A. Suarez, G. Gilardoni, L. Cartuche, P. Flores, V. Morocho, *Mol. Ther.* **2016**, *21*, 1461.
[67] H. Teng, L. Chen, T. Fang, B. Yuan, Q. Lin, *J. Funct. Foods* **2017**, *28*, 306.
[68] S. Kozuch, S. Shaik, *Acc. Chem. Res.* **2011**, *44*, 101.

How to cite this article: Sujayev A, Taslimi P, Kaya R, et al. Synthesis, characterization and biological evaluation of *N*-substituted triazinane-2-thiones and theoretical–experimental mechanism of condensation reaction. *Appl Organometal Chem*. 2019;e5329. https://doi.org/10.1002/aoc.5329